J. Chem. Sci., Vol. 117, No. 5, September 2005, pp. 573–582.

Bottlenecks in the prediction of regioselectivity of [4 + 2] cycloaddition reactions: An assessment of reactivity descriptors

G GAYATRI and G NARAHARI SASTRY*

Molecular Modeling Group, Organic Chemical Sciences, Indian Institute of Chemical Technology, Hyderabad 500 007, India
e-mail: gnsastry@iict.res.in

Abstract. B3LYP/6-31G(*d*) calculations were performed to obtain all the transition states and products for the 128 distinct reaction channels of Diels–Alder reactions by taking all possible combinations from a series of dienes (1N-a, 1N-b, 2N, 1P-a, 1P-b, 2P, 1O, 1S) and dienophiles (NE, PE, OE, SE, AE, OHE, MeE, CNE). The predictive ability of the values to gauge the regioselectivity of the putative [4 + 2] cycloaddition reactions is analysed. No correlation is obtained between the reaction energies and activation energies. The extent of asynchronicity is measured based on the bond order analysis. DFT-based descriptors such as the local softness (s_k^+ and s_k^-), Fukui function indices (f_k^+ and f_k^-), global electrophilicity index (w) and local electrophilicity index (w_k) were found to be better than the conventional FMO predictions.

Keywords. Prediction of regioselectivity; [4 + 2] cycloaddition reactions; reactivity descriptors; DFT-based descriptors.

1. Introduction

Cycloaddition reactions, Diels–Alder reactions in particular, are the most general protocols employed to access novel and complex heterocyclic compounds.[1] When more than one possible coupling routes is available, the mechanism of transition state formation differs for different orientations of coupling, thereby preferring one over the other. In synthetic chemistry, regioselectivity has been one of the most important aspects to keep in mind and understanding the factors controlling regioselectivity helps a great deal in synthetic strategies. A quick perusal of the combined experimental and computational studies reveal that prediction of regioselectivity in cycloaddition reactions is still a challenging task and no reliable criterion exists which explains all the expected observations involving regioselectivity.[1] The frontier molecular orbital model has been the most popular among the predictive models of regioselectivity in pericyclic reactions. In addition, local hard and soft acid base (HSAB) principles have been also employed to predict the observed regioselectivity.[2] In recent years, the conceptual density functional theory has been remarkably successful in explaining the reactivity and site selectivity.[3] The density functional theory based reactivity descriptors thus obtained are helpful to model the regioselectivity in cycloaddition reactions. The descriptors we have chosen to scrutinize their ability to estimate the regioselectivity are Fukui function indices (f_k^+ and f_k^-), global softness (S), local softness (s_k^+ and s_k^-), global electrophilicity index (w) and local electrophilicity index (w_k^+ and w_k^-).[4] Bond order analysis is also done to understand the synchronous and asynchronous behavior of the reactant pair.[5]

The mechanism of the Diels–Alder reaction was a subject of controversy until about a decade ago.[6] Now there is a consensus that both concerted and stepwise paths exist and the former pathway is more preferred in most instances.[7] Although there are exceptions of stepwise path overtaking the concerted, in situations where the substituents stabilize the radical intermediate, such possibility appears to be remote in the diene–dienophile combinations considered here. Therefore, only the concerted pathway is considered in the present study. It is to be mentioned that the conventional *ab initio* methods have great difficulty in estimating the activation energy barriers. While the Hartree–Fock method substantially overestimates the activation barrier, MP2 underestimation is also equally bad.[8] The recent benchmark study reveal that B3LYP method, even with 6-31G(*d*) basis set, appears to be the best compromise to model Diels–Alder reactions involving medium-sized molecules. In addition, this method is a test on a variety of diene–dienophile combinations and seems to be working extremely well.[9]

*For correspondence

In this paper, we have examined the performance of various qualitative models to explain the regioselectivity by taking a series of idealized diene-dienophile reactant pairs. A total of 64 reactions are considered, which essentially leads to probing of 128 reaction channels. All the transition states are located and characterized at B3LYP/6-31G(*d*) level and the activation barrier thus obtained is taken as a reference for the reaction feasibility.

2. Methodology and computational details

Geometry optimizations and frequency calculations were done on the reactants, transition states and products using the hybrid density functional theory, B3LYP with 6-31G(*d*) basis set, as B3LYP has been proved to be a better method and 6-31G(*d*) a better basis set to evaluate the above descriptors. The frequency calculations suggest that reactants and products possess zero imaginary frequency and the transition states are a stationary point with one imaginary frequency. As attempts to locate the transition states, 1P-a-2PE, 1P-b-1PE, 1P-a-1OE, 1N-b-2SE, 1P-a-1SE, 1P-a-2SE and 1P-b-1SE, were futile at B3LYP level, transition state energies were evaluated on geometries obtained at AM1 level. Bond orders are calculated on B3LYP/6-31G(d) optimized geometries using Gamess program package.[10] Mulliken populations were used for the charges. All the calculations were done using Gaussian 98W program.[11]

A brief description of the definitions and computations of the density functional theory based descriptors and synchronicity parameters used in the study is as follows. Fukui function was introduced by Parr and coworkers based on the frontier orbital concept given by Fukui.[3,12] It is defined as the derivative of electron density $r(r)$ with respect to the total number of electrons, N, in the system at a constant external potential $v(r)$ acting on an electron due to all the nuclei present in the system.

Later, Yang and Mortier extended the term Fukui function and proposed the condensed form of Fukui functions at a particular atom, k, in a molecule with N electrons. This leads to Fukui function indices for different classes of reactions as follows

$$f_k^+ = [q_k(N + 1) - q_k(N)]$$

for nucleophilic attack (1)

$$f_k^- = [q_k(N) - q_k(N-1)]$$

for electrophilic attack (2)

$$f_k^\bullet = [q_k(N + 1) - q_k(N - 1)]$$

for free radical attack. (3)

Global softness (S) is another important descriptor, which helps in explaining the reactivity patterns. Global softness is given by

$$S = 1/e_{\mathrm{LUMO}} - e_{\mathrm{HOMO}}. \quad (4)$$

Local softness, $s(r)$, is another parameter which gives the softness at a particular site, k, in a molecule. It is given by

$$s_k^+ = Sf_k^+, \quad \text{for nucleophilic attack,} \quad (5)$$

$$s_k^- = S f_k^- \quad \text{for electrophilic attack,} \quad (6)$$

$$s_k^\bullet = S f_k^\bullet \quad \text{for free radical attack.} \quad (7)$$

Electrophilicity index (w) in normal terms is defined as the electrophilic power of a ligand or the capability of an agent to accept electrons. It can also be defined as a measure of lowering the energy due to the maximum flow of electrons. All the DFT-based descriptors are obtained by substituting the frontier orbital energy values and charge densities obtained from B3LYP/6-31G* calculations done with Gaussian program package. The global electrophilicity index is given by

$$w = m^2/2h, \quad (8)$$

where $m = (e_{\mathrm{HOMO}} + e_{\mathrm{LUMO}})$ and $h = \varepsilon_{\mathrm{LUMO}} - e_{\mathrm{HOMO}}$.

The local electrophilicity index (w_k), which gives the maximum electrophilicity power in a molecule developed at a particular site, is given by

$$w_k^+ = f_k^+, \quad \text{for nucleophilic attack,} \quad (9)$$

$$w_k^- = f_k^-, \quad \text{for electrophilic attack,} \quad (10)$$

$$w_k^\bullet = w f_k^\bullet, \quad \text{for free radical attack,} \quad (11)$$

Using the bond orders, synchronicity (Sy) of a the reaction is calculated by the following equation[13]

$$Sy = 1 - \left\{ \sum_{i=1}^{n} \left| \frac{dB_i - dB_{av}}{dB_{av}} \right| \right\} \Big/ (2n - 2), \quad (12)$$

where n is the number of bonds directly involved in the reaction and dB_i is the relative variation of the bond order index B_i at the transition state and is given as follows

$$dB_i = \frac{B_i^{TS} - B_i^{R}}{B_i^{P} - B_i^{R}}, \tag{13}$$

where TS, R and P refer to the transition state, reactant and product respectively. The $\ddot{a}B_{av}$ is given by

$$dB_{av} = \frac{1}{n}\sum_{i=1}^{n} dB_i. \tag{14}$$

A complete reactivity analysis on Diels–Alder reactions is performed using the above parameters.

3. Results and discussion

In this section we start with the description of computed activation and reaction energies for all the reaction paths considered. Then, we seek to explore whether there is a correlation between the activation and reaction energies.[14] The effect of asynchronocity of the transition state structures on the regioselectivity and reaction feasibility is assessed next. This is followed by an evaluation of the predictive ability of the frontier molecular orbital (FMO) and the conceptual DFT based descriptors for the regioselectivity in the reactions.

Table 1 gives the activation energies, reaction energies, synchronicities and the distances at the transition state for the twin bonds to be formed (see scheme 1). Among the 64 combinations, 39 reactions showed head-to-tail coupling (1–2′, see scheme 2) and 25 reactions showed head-to-head (1–1′) coupling. The optimized geometries of all the dienes and dienophiles considered in the study are given in figures 1 and 2 respectively. Among the dienophiles considered, phosphine, PE, is the best dienophile, with low activation energies and higher exothermicities compared to the rest. In contrast, formaldehyde, OE, is the poorest among the dienophiles considered. However, the data indicate that such clear demarcation of reactivity, based on the dienes, is not possible. The collected data indicate that activation barriers range from virtually barrierless reactions to more than 40 kcal/mol. While most reactions are exothermic (124 out of 128), some exceptions do exist. A comparison of forming bond distance at the transition state indicates that some of the reactions are highly asynchronous. Considering that the atom types are very different in the transition state, a more reliable bond order-based asynchronicity measure was taken to quantify the unsymmetrical nature of the concerted transition states. Obviously, at least for some of the reactions, the alternate stepwise reaction mechanism may be more favorable, but as the focus of the paper is to assess the performance of the reactivity measures for the pericyclic reactions, we restrict ourselves here to only the concerted pathway. As the dienophile type appears to control the reactivity the discussion is arranged accordingly.

3.1 *Reaction exothermicitiy and activation energies*

Exothermicity of a reaction has been one of the most important factors to determine the reaction feasibility. Previous studies reveal that there exists a good linear correlation between the reaction exothermicity and activation energies in some class of Diels–Alder reactions. Figure 3 depicts the plot of correlation between the reaction energies and exothermicities. Surprisingly, there is hardly any correlation, thereby the thermodynamic and kinetic factors are entirely different and work in opposite directions in some cases. The

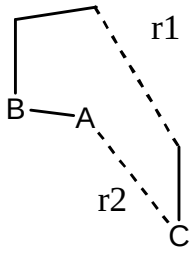

Scheme 1.

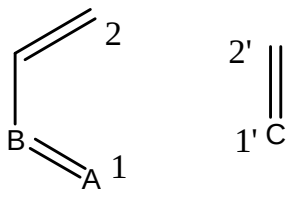

A = –NH, –PH, –O, –S, –CH_2
B = –N, –P, –CH
C = –NH, –PH, –O, –S, –CHMe, –CHOH, CHCN, CHCHO

Scheme 2.

Table 1. Activation energies and reaction energies (in kcal/mol), synchronicity (in a.m.u.), bond forming transition state distances, $r1$ and $r2$ (in Å) for [4 + 2] cycloaddition reactions at B3LYP/6-31G* level.

No.	Diene	Dienophile	Reaction	$\Delta E^{\ddagger}$	ΔE_r	*Sy*	$r1$	$r2$
1	1N-a	NE	1N-a-1′NE	29·9	–10·9	0·923	2·000	2·091
2			1N-a-2′CH_2E	14·1	–23·5	0·881	1·963	2·316
3	1N-b		1N-b-1′NE	31·4	–13·8	0·870	1·849	2·234
4			1N-b-2′CH_2E	19·5	–25·4	0·793	1·812	2·610
5	2N		2N-1′NE	13·8	–37·5	0·851	2·599	1·907
6			2N-2′CH_2E	19·3	–34·2	0·898	2·023	2·355
7	1P-a		1P-a-1′NE	10·3	–34·3	0·812	2·651	2·195
8			1P-a-2′CH_2E	9·7	–27·9	0·918	2·059	2·794
9	1P-b		1P-b-1′NE	8·2	–38·5	0·806	2·638	2·176
10			1P-b-2′CH_2E	11·5	–27·9	0·903	2·019	2·897
11	2P		2P-1′NE	14·2	–34·8	0·623	2·960	1·948
12			2P-2′CH_2E	18·1	–35·4	0·862	1·947	2·513
13	1O		1O-1′NE	35·5	8·3	0·861	1·797	2·095
14			1O-2′CH_2E	11·6	–17·3	0·819	1·906	2·438
15	1S		1S-1′NE	16·7	–22·6	0·925	2·239	2·253
16			1S-2′CH_2E	5·0	–24·6	0·900	2·124	2·882
17	1N-a	PE	1N-a-1′PE	9·1	–43·8	0·907	2·439	2·388
18			1N-a-2′CH_2E	9·4	–32·6	0·895	2·493	2·339
19	1N-b		1N-b-1′PE	13·6	–44·3	0·930	2·343	2·415
20			1N-b-2′CH_2E	12·4	–33·5	0·861	2·299	2·423
21	2N		2N-1′PE	8·5	–43·8	0·907	2·583	2·544
22			2N-2′CH_2E	8·0	–42·2	0·895	2·637	2·556
23	1P-a		1P-a-1′PE	3·6	–45·8	0·773	3·021	3·105
24			1P-a-2′CH_2E	33·7[a]	–39·0	0·910	2·390	2·384
25	1P-b		1P-b-1′PE	28·4[a]	–47·4	0·698	2·916	2·246
26			1P-b-2′CH_2E	3·2	–40·7	0·906	2·846	3·055
27	2P		2P-1′PE	6·9	–46·5	0·689	2·911	2·455
28			2P-2′CH_2E	9·0	–43·3	0·893	2·626	2·506
29	1O		1O-1′PE	12·0	–38·3	0·941	2·298	2·357
30			1O-2′CH_2E	10·8	–22·9	0·844	2·309	2·299
31	1S		1S-1′PE	3·4	–47·0	0·811	2·791	2·921
32			1S-2′CH_2E	2·5	–34·9	0·877	2·837	2·998
33	1N-a	OE	1N-a-1′OE	31·8	6·8	0·878	2·828	2·037
34			1N-a-2′CH_2E	16·8	–20·6	0·901	2·090	1·875
35	1N-b		1N-b-1′OE	35·1	6·3	0·866	1·737	2·091
36			1N-b-2′CH_2E	27·3	–23·2	0·938	1·916	2·038
37	2N		2N-1′OE	17·2	–33·5	0·926	2·113	2·070
38			2N-2′CH_2E	23·5	–29·2	0·938	2·106	2·035
39	1P-a		1P-a-1′OE	32·5[a]	–38·2	0·765	2·658	2·198
40			1P-a-2′CH_2E	14·0	–23·4	0·935	2·037	2·441
41	1P-b		1P-b-1′OE	12·9	–34·5	0·930	2·224	2·294
42			1P-b-2′CH_2E	17·1	–21·8	0·924	2·028	2·416
43	2P		2P-1′OE	23·3	–29·0	0·917	2·190	1·997
44			2P-2′CH_2E	20·2	–31·2	0·847	2·194	2·007
45	1O		1O-1′OE	44·3	33·4	0·887	1·656	1·850
46			1O-2′CH_2E	16·2	–15·6	0·942	1·924	1·950
47	1S		1S-1′OE	20·9	–11·5	0·893	2·015	2·282
48			1S-2′CH_2E	8·6	–21·1	0·946	2·016	2·488
49	1N-a	SE	1N-a-1′SE	11·1	–23·9	0·916	2·175	2·458
50			1N-a-2′CH_2E	5·52	–32·1	0·866	2·724	2·081
51	1N-b		1N-b-1′SE	15·2	–27·2	0·854	2·061	2·627
52			1N-b-2′CH_2E	20·2[a]	–34·7	0·880	1·889	2·189

(*contd…*)

Table 1. (*contd…*)

No.	Diene	Dienophile	Reaction	$\Delta E^{\ddagger}$	ΔE_r	*Sy*	*r*1	*r*2
53	2N		2N-1′SE	8·1	–43·0	0·916	2·361	2·673
54			2N-2′CH_2E	8·9	–41·5	0·937	2·603	2·358
55	1P-a		1P-a-1′SE	27·8[a]	–48·7	0·858	2·440	2·357
56			1P-a-2′CH_2E	35·0[a]	–37·4	0·653	2·410	2·949
57	1P-b		1P-b-1′SE	22·0[a]	–45·5	0·873	2·320	2·337
58			1P-b-2′CH_2E	3·1	–36·5	0·906	2·733	2·796
59	2P		2P-1′SE	7·7	–43·5	0·717	2·737	2·334
60			2P-2′CH_2E	8·1	–42·3	0·823	2·781	2·295
61	1O		1O-1′SE	16·7	–13·3	0·863	2·026	2·415
62			1O-2′CH_2E	8·9	–24·2	0·920	2·354	2·081
63	1S		1S-1′SE	5·4	–36·7	0·912	2·431	2·806
64			1S-2′CH_2E	1·0	–32·9	0·922	2·803	2·848
65	1N-a	AE	1N-a-1′AE	20·4	–31·1	0·889	2·052	2·304
66			1N-a-2′CH_2E	19·2	–29·9	0·878	2·393	1·972
67	1N-b		1N-b-1′AE	26·6	–32·9	0·826	1·930	2·497
68			1N-b-2′CH_2E	27·0	–29·1	0·777	2·260	2·031
69	2N		2N-1′AE	18·2	–39·2	0·920	2·201	2·393
70			2N-2′CH_2E	19·2	–38·8	0·939	2·471	2·130
71	1P-a		1P-a-1′AE	13·3	–33·6	0·929	2·268	2·725
72			1P-a-2′CH_2E	11·8	–33·2	0·865	2·525	2·453
73	1P-b		1P-b-1′AE	14·8	–33·9	0·921	2·243	2·758
74			1P-b-2′CH_2E	13·6	–33·8	0·873	2·491	2·444
75	2P		2P-1′AE	21·1	–40·4	0·906	2·204	2·389
76			2P-2′CH_2E	18·4	–39·3	0·752	2·697	2·078
77	1O		1O-1′AE	23·9	–19·9	0·842	1·945	2·278
78			1O-2′CH_2E	23·7	–21·1	0·931	2·138	2·005
79	1S		1S-1′AE	13·5	–29·9	0·915	2·191	2·695
80			1S-2′CH_2E	11·9	–30·8	0·906	2·356	2·461
81	1N-a	OHE	1N-a-1′OHE	18·4	–34·3	0·893	2·029	2·331
82			1N-a-2′CH_2E	27·0	–30·3	0·959	2·191	2·130
83	1N-b		1N-b-1′OHE	22·2	–36·1	0·854	1·979	2·453
84			1N-b-2′CH_2E	30·9	–32·0	0·944	2·147	2·147
85	2N		2N-1′OHE	22·2	–41·7	0·931	2·204	2·345
86			2N-2′CH_2E	18·9	–41·4	0·864	2·587	2·022
87	1P-a		1P-a-1′OHE	14·2	–34·0	0·921	2·113	2·859
88			1P-a-2′CH_2E	15·1	–36·0	0·863	2·513	2·384
89	1P-b		1P-b-1′OHE	16·1	–34·5	0·917	2·110	2·935
90			1P-b-2′CH_2E	14·7	–36·4	0·842	2·535	2·309
91	2P		2P-1′OHE	22·8	–43·4	0·893	2·114	2·462
92			2P-2′CH_2E	19·3	–42·2	0·683	2·865	1·992
93	1O		1O-1′OHE	14·6	–30·8	0·856	1·997	2·341
94			1O-2′CH_2E	28·8	–22·3	0·924	2·042	2·126
95	1S		1S-1′OHE	9·0	–33·6	0·895	2·116	2·958
96			1S-2′CH_2E	15·6	–32·3	0·922	2·309	2·469
97	1N-a	MeE	1N-a-1′MeE	20·9	–36·9	0·923	2·128	2·257
98			1N-a-2′CH_2E	23·7	–34·2	0·944	2·185	2·163
99	1N-b		1N-b-1′MeE	25·2	–36·5	0·891	2·011	2·376
100			1N-b-2′CH_2E	23·2	–34·0	0·939	2·185	2·163
101	2N		2N-1′MeE	20·1	–44·7	0·944	2·306	2·254
102			2N-2′CH_2E	19·5	–43·2	0·924	2·435	2·143
103	1P-a		1P-a-1′MeE	14·3	–38·9	0·942	2·294	2·646
104			1P-a-2′CH_2E	14·1	–37·8	0·912	2·410	2·517
105	1P-b		1P-b-1′MeE	15·6	–39·2	0·939	2·279	2·651
106			1P-b-2′CH_2E	14·7	–38·5	0·896	2·429	2·478

(*contd…*)

Table 1. (*contd…*)

No.	Diene	Dienophile	Reaction	$\Delta E^{\ddagger}$	ΔE_r	*Sy*	*r*1	*r*2
107	2P		2P-1′MeE	22·1	–45·3	0·913	2·309	2·275
108			2P-2′CH_2E	20·8	–43·6	0·803	2·562	2·105
109	1O		1O-1′MeE	19·6	–30·0	0·875	2·014	2·269
110			1O-2′CH_2E	24·8	–26·3	0·915	2·049	2·269
111	1S		1S-1′MeE	11·5	–37·5	0·935	2·210	2·715
112			1S-2′CH_2E	13·2	–36·0	0·945	2·270	2·572
113	1N-a	CNE	1N-a-1′CNE	21·1	–31·2	0·873	2·031	2·330
114			1N-a-2′CH_2E	20·1	–31·6	0·884	2·393	1·961
115	1N-b		1N-b-1′CNE	24·7	–30·8	0·815	1·914	2·526
116			1N-b-2′CH_2E	27·0	–32·9	0·922	2·332	1·976
117	2N		2N-1′CNE	18·2	–42·0	0·900	2·168	2·438
118			2N-2′CH_2E	18·9	–40·8	0·905	2·512	2·089
119	1P-a		1P-a-1′CNE	13·9	–36·2	0·932	2·218	2·777
120			1P-a-2′CH_2E	12·3	–34·6	0·863	2·544	2·423
121	1P-b		1P-b-1′CNE	14·5	–36·5	0·929	2·210	2·804
122			1P-b-2′CH_2E	13·7	–36·1	0·867	2·525	2·394
123	2P		2P-1′CNE	21·0	–42·7	0·901	2·148	2·448
124			2P-2′CH_2E	17·9	–41·9	0·729	2·784	2·034
125	1O		1O-1′CNE	23·1	–21·2	0·831	1·932	2·295
126			1O-2′CH_2E	25·0	–22·6	0·939	2·165	1·977
127	1S		1S-1′CNE	13·6	–30·9	0·909	2·167	2·725
128			1S-2′CH_2E	13·1	–31·7	0·902	2·371	2·425

[a]Calculations at B3LYP/6-31G*//AM1 level

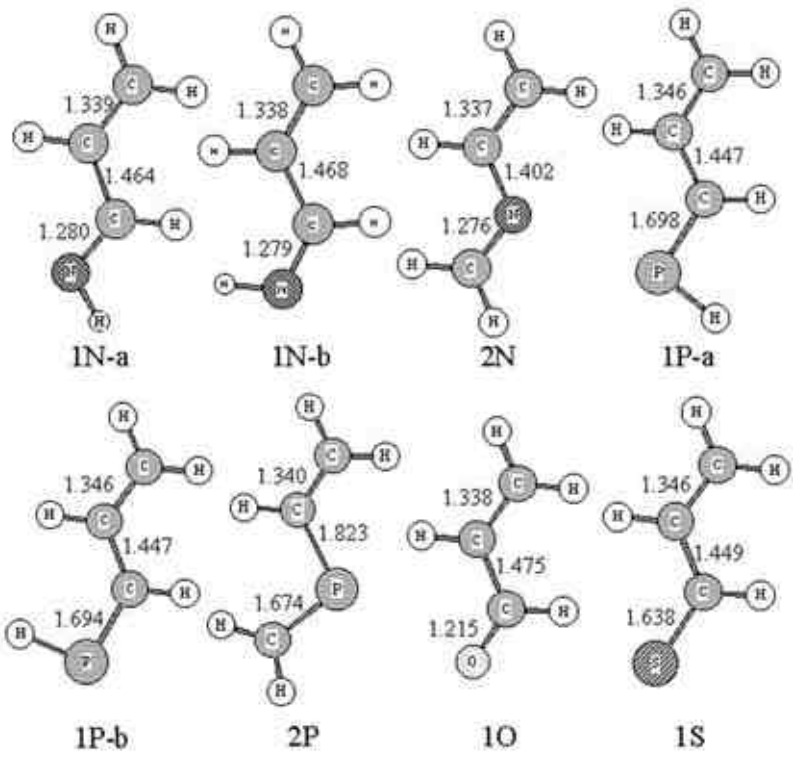

Figure 1. B3LYP/6-31G* optimized geometries of dienes.

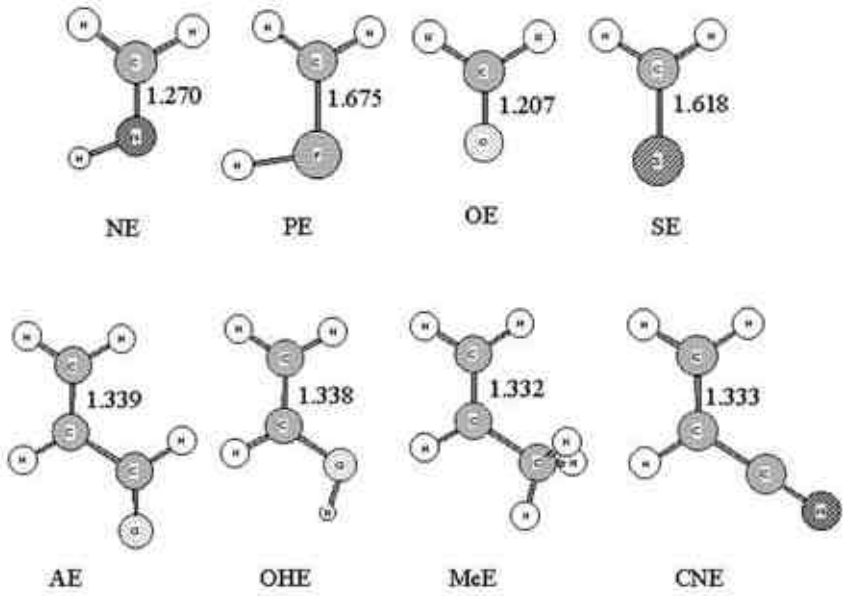

Figure 2. B3LYP/6-31G* optimized geometries of dienophiles.

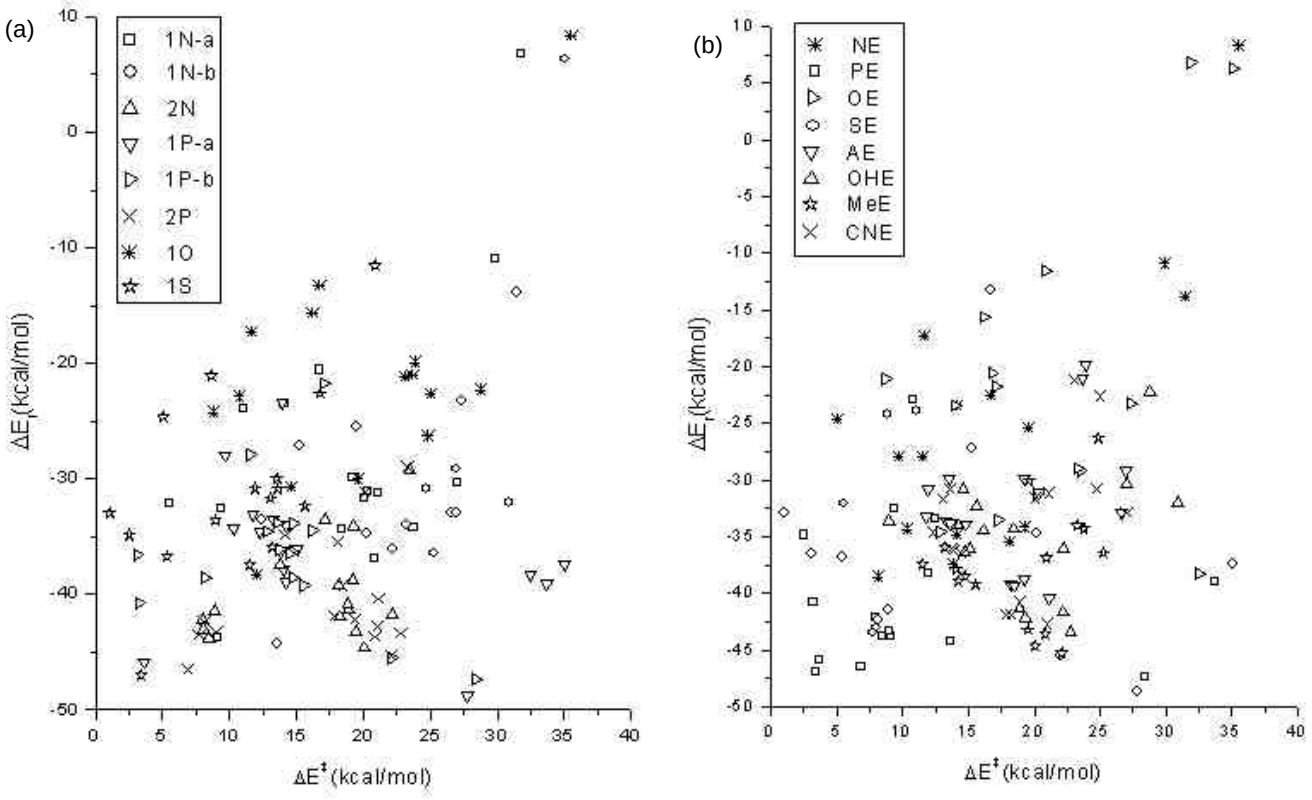

Figure 3. Plot of reaction energies vs activation energies with reference to dienes (**a**), and to dienophiles (**b**).

activation energy ranges vary quite widely for reactions with similar reaction energies. While exothermicity still appears to be a very useful indicator of regioselectivity, it is not yet a foolproof criterion. As many as 25 examples, although the magnitude is small in a majority of cases, were encountered among the models considered where the regioselectivity is on the opposite side of the reaction energy. However, in cases of 1N-

b and PE, 1O and PE, 1S and PE, and 1P-a and OE, the regioisomer, which is more stable by about 10–17 kcal/mol, has the higher barrier! Therefore, prediction of the reactivity of the Diels–Alder reaction and regioselectivity is too complicated to be done using the reaction exothermicities.

3.2 *Reaction asynchronicity and regioselectivity*

Equation (17) is employed to compute the synchronicity of the transition states with the help of bond orders calculated using the GAMESS program package. Among the 64 reactions considered, the activation barrier for head-to-head (1–1′) is lower in 25 cases while head-to-tail (1–2′) coupling is preferred in the other 39 cases. The reactions paths, which are more asynchronous, have lower activation barrier in 45 out of the 64 cases. However, when OE and S are the dienophiles, 10 out of 16 reactions have lower barriers for the more synchronous transition state, which is in contrast with the regular trend.

The foregoing analysis indicates that prediction of regioselectivity is an intricate task and that there are several factors in concordance and discordance which eventually decide the preferred orientation of coupling. Reaction exothermicity, synchronicity, the type of electron demand and the activation of the twin regioisomer pathways are largely independent. With this background, we venture to assess the density functional and frontier molecular orbital theory based descriptors for their predictive ability of regioselectivity in Diels–Alder reactions.

3.3 *Frontier molecular orbital (FMO) analysis*

Table 2 gives the frontier orbital energy values along with the coefficients of the dienes and dienophiles. Thus, while NE, OHE, MeE prefer the inverse electron demand, the rest appear to follow the normal electron demand. This demand refers to a situation where the donating group is a diene, while inverse electron demand refers to a situation when a dienophile is the donating group. According to the frontier orbital energy analysis, the type of electron demand is mostly controlled by the dienophile type. Thus, reactions involving NE, OHE, and MeE follow the inverse electron demand, while the rest are in the category of reactions with normal electron demand. While the type of electron demand does not correlate with the activation energy or regioselectivity, the frontier orbital gaps correlate well with activation energies. However, the regioselectivity has to be controlled by the orbital coefficients at the reaction centres. However, careful analyses indicate that most of the reactions (35 out of 64) do not follow the prediction of frontier molecular orbital theory. Thus, frontier orbital theory-based arguments have a very low success rate in predicting the regioselectivity of Diels–Alder reactions.

3.4 *Density functional theory based descriptors*

Table 3 provides the local softness (s_k^+ and s_k^-), Fukui functions (f_k^+ and f_k^-), global softness (S), global electrophilicity index (w) and local electrophilicity index (w_k^+ and w_k^- in electron volts) for the dienes and dienophiles considered. According to the global electrophilicity index scale,[4c] the values obtained in the present study indicate that all the dienes and the dienophiles, PE, OE, SE, AE and CNE are strong electrophiles, while the dienophiles NE, OHE and MeE are marginal electrophiles. Thus, there is competition between the dienes and dienophiles for electron acceptance. Hence, we have considered both the possibilities, i.e. dienes are considered to be acting as nucleophiles and the dienophiles to be electrophiles in the first case, and vice versa, in the second case. Larger values of local DFT-based descriptors are observed at the reactive sites for both the dienes and dienophiles. When we consider the f_k^- values for diene and f_k^+ values for dienophile (f_k^-/f_k^+), the regioselectivity can be successfully explained in about 38 out of the 64 model systems considered in the study. Interestingly, when f_k^+ of diene and f_k^- of dienophile (f_k^+/f_k^-) is taken as a measure, the success of predictive ability rises sharply, and here the regioselectivity is correctly explained in as many as 43 cases. As categorizing dienes and dienophiles strictly into electrophiles and nucleophiles is difficult, the choice

Table 2. HOMO and LUMO values (in eVs) for the dienes and dienophiles.

Diene	HOMO	LUMO	Dienophile	HOMO	LUMO
1N-a	7·13	1·23	NE	7·29	0·26
1N-b	7·21	1·26	PE	7·36	1·70
2N	6·79	1·04	OE	7·31	1·15
1P-a	6·34	2·07	SE	6·35	2·57
1P-b	6·38	2·09	AE	7·00	1·77
2P	6·56	1·64	OHE	6·06	1·19
1O	7·00	1·77	MeE	6·75	0·58
1S	6·10	2·72	CNE	7·87	1·53

Table 3. f_k^+ and f_k^-, global softness (S), local softness (s_k^+ and s_k^-) in a.m.u., global electrophilicity index (w) and local electrophilicity index (w_k^+ and w_k^- in eVs for the dienes and the dienophiles considered. All calculations are done at B3LYP/6-31G* level.

		Orbital coefficients	f_k^+	f_k^-	w	S	w_k^+	w_k^-	s_k^+	s_k^-
Dienes										
1N-a	1	–0·32	0·274	0·428	1·42	4·53	0·389	0·608	1·240	1·940
	2	0·37	0·374	0·247			0·536	0·351	1·692	1·121
1N-b	1	–0·33	0·270	0·421	1·51	4·58	0·407	0·636	1·233	1·928
	2	0·36	0·384	0·260			0·580	0·393	1·759	1·191
2N	1	–0·28	0·421	0·380	1·33	4·73	0·560	0·506	1·990	1·797
	2	0·38	0·356	0·237			0·474	0·315	1·684	1·119
1P-a	1	–0·16	0·511	0·488	2·07	6·37	1·060	1·013	3·257	3·112
	2	–0·32	0·291	0·321			0·604	0·666	1·856	2·048
1P-b	1	–0·16	0·513	0·492	2·09	6·34	1·069	1·026	3·248	3·116
	2	–0·31	0·293	0·319			0·612	0·664	1·859	2·019
2P	1	0·36	0·304	0·308	1·71	5·53	0·518	0·525	1·678	1·703
	2	–0·28	0·272	0·308			0·463	0·524	1·502	1·701
1O	1	–0·28	0·191	0·366	1·84	5·20	0·351	0·673	0·994	1·906
	2	0·38	0·390	0·273			0·716	0·501	2·027	1·418
1S	1	–0·18	0·455	0·615	2·87	8·04	1·304	1·765	3·655	1·947
	2	–0·32	0·312	0·237			0·895	0·681	2·509	1·908
Dienophiles										
NE	1′	–0·45	0·390	0·508	1·01	3·87	0·395	0·515	1·507	1·967
	2′	0·46	0·610	0·492			0·619	0·498	2·361	1·902
PE	1′	0·17	0·638	0·691	1·81	4·81	1·156	1·252	3·069	3·324
	2′	0·43	0·362	0·309			0·656	0·560	1·742	1·487
OE	1′	–0·44	0·276	0·434	1·45	4·42	0·400	0·629	1·217	1·915
	2′	0·50	0·725	0·567			1·050	0·821	3·200	2·503
SE	1′	0·18	0·575	0·694	2·64	7·21	1·516	1·831	4·147	5·007
	2′	0·47	0·425	0·306			1·120	0·806	3·064	2·204
AE	1′	–0·22	0·154	0·113	1·84	5·20	0·282	0·207	0·799	0·585
	2′	0·38	0·390	0·273			0·715	0·501	2·026	1·418
OHE	1′	0·48	0·364	0·243	0·41	3·75	0·149	0·149	1·364	1·364
	2′	–0·39	0·487	0·475			0·199	0·199	1·828	1·828
MeE	1′	–0·42	0·229	0·256	0·65	3·72	0·149	0·149	0·852	0·852
	2′	0·39	0·459	0·463			0·298	0·298	1·704	1·704
CNE	1′	–0·32	0·256	0·241	1·74	4·29	0·446	0·420	1·099	1·034
	2′	0·42	0·429	0·387			0·748	0·675	1·841	1·662

between the above two criteria is not straightforward. However, it is very clear that the success rate of regioselectivity prediction is much higher with any of the DFT-based descriptors compared to conventional FMO-based descriptors, which predict the correct regioselectivity only in 29 out of 64 cases. For example, considering the reactions of all the dienes with NE, NE has f_k^+/f_k^- values for the sites 1′ and 2′ equal to 0·390/0·508 and 0·610/0·492. When the reaction between 1N-a and NE is considered, the f_k^+/f_k^- values for the sites 1 and 2 of 1N-a are 0·274/0·428 and 0·374/0·247. This values indicate that 1–2′ coupling is more favorable whether one considers either the f_k^+ or the f_k^- values of the dienophile. Essentially the same situation exists for the reactions with 1N-b and 1O, which bear the f_k^+/f_k^- values 0·270/0·421 and 0·384/0·260, and 0·191/0·366 and 0·390/0·273 for the sites 1 and 2 respectively. When the reactions with 2N is considered, the f_k^+/f_k^- values at the sites 1 and 2 are 0·421/0·380 and 0·356/0·237. The values suggest the formation of most favorable product only when f_k^- values of dienophile are considered. Same is the case with 1P-b and 2P bearing the f_k^+/f_k^- values of 0·513/0·492 and 0·293/0·319, and 0·304/0·308 and 0·272/0·308 at the sites 1 and 2 respectively. In contrast, in 1P-a has f_k^+/f_k^- values of 0·511/0·488 and 0·291/0·321 at the sites 1 and 2 respectively, which lead us to consider only the f_k^+ values of dienophile.

Thus, when such heteromolecular couplings are considered, a combined analysis was adopted in ascertaining the nature of the reactions. The local electrophilicity indices and local softness values follow essentially the same trend. It was found that in only 11 out of the 64 cases, neither (f_k^-/f_k^+) nor (f_k^+/f_k^-) measures could explain the observed regioselectivity. The consistency of the Fukui function, electrophilicity and softness indices makes them very similar reactivity measures in predicting the regioselectivity. Thus when DFT measures are applied to regioselectivity any one of the measures seems to be sufficient.

4. Conclusions

A systematic computational study is undertaken to understand the regioselectivity in cycloaddition reactions. About 64 combinations of reactant pairs were taken, where each pair has the possibility of forming two distinct regioisomers. B3LYP/6-31G(*d*) calculations were performed to obtain the activation and reaction energies for all the systems studied. The frontier orbital model has shown very severe limitations in predicting the regioselectivity. In comparison, DFT-based descriptors are better suited to model the regioselectivity of cycloaddition reactions.

Acknowledgements

GG thanks the Council of Scientific and Industrial Research for a fellowship.

References

1. Winkler J D 1996 *Chem. Rev.* **96** 167; Chen Z and Trundell M L 1996 *Chem. Rev.* **96** 1179; Vogel P, Cossy J, Plumet J and Arjona O 1999 *Tetrahedron* **55** 13521; Boger D L 1986 *Chem. Rev.* **86** 781
2. Parr R G and Pearson R G 1983 *J. Am. Chem. Soc.* **105** 7512; Chattaraj P K, Lee H and Parr R G 1991 *J. Am. Chem. Soc.* **113** 1855; Liu S and Parr R G 1997 *J. Chem. Phys.* **106** 5578
3. Geerlings P, Proft F D and Langenaeker W 2003 *Chem. Rev.* **103** 1793; Roy R K, Krishnamurti S, Geerlings P and Pal S 1998 *J. Phys. Chem.* **A102** 3746; Mendez F, Tamariz J and Geerlings P 1998 *J. Phys. Chem.* **A102** 6292; Yang W and Mortier W J 1986 *J. Am. Chem. Soc.* **108** 5708; Parr R G and Yang W 1984 *J. Am. Chem. Soc.* **106** 4049
4. Nguyen L T, Proft F de, Dao V L, Nguyen M T and Geerlings P 2003 *J. Phys. Org. Chem.* **16** 615; Domingo R L, Jose Aurell M, Perez P and Renato R C 2003 *J. Org. Chem.* **68** 3884; Domingo R L, Aurell M J, Perez P and Contreras R 2002 *Tetrahedron* **58** 4417; Domingo L R, Oliva M and Andres J 2001 *J. Mol. Struct.* (*Theochem.*) **554** 79; Domingo L R, Perez P and Contreras R 2004 *Tetrahedron* **60** 6585; Sengupta D, Chandra A K and Nguyen M T 1997 *J. Org. Chem.* **62** 6404; Sivanesan D, Amutha R, Subramanian V, Nair B U and Ramasami T 1999 *Chem. Phys. Lett.* **308** 223; Roy R K, Pal S and Hirao K 1999 *J. Chem. Phys.* **110** 8236; Padmanabhan J, Parthasarathi R, Sarkar U, Subramanian V and Chattaraj P K 2004 *Chem. Phys. Lett.* **383** 122; Chattaraj P K, Maiti B and Sarkar U 2003 *J. Phys. Chem*. **A107** 4973; Domingo R L, Jose Aurell M, Perez P and Renato R C 2002 *J. Phys. Chem.* **A106** 6871; Jose Aurell M, Domingo R L, Perez P and Renato R C 2004 *Tetrahedron* **60** 11503
5. Punnagai M, Dinadayalane T C and Sastry G N 2004 *J. Phys. Org. Chem.* **17** 152; Lee C, Yang W and Parr R G 1988 *Phys. Rev.* **B37** 785; Hernandez-Garcia R M, Barba-Behrens N, Salcedo R and Hojer G 2003 *J. Mol. Struct.* (*Theochem.*) **637** 55; Lim C C, Xu Z P, Huang H H, Mok C Y and Chin W S 2000 *Chem. Phys. Lett.* **325** 433; Vijaya R and Sastry G N 2002 *J. Mol. Struct.* (*Theochem.*) **618** 201
6. Beno B R, Wilsey S and Houk K N 1999 *J. Am. Chem. Soc.* **121** 4816; Horn B A, Herek J L and Zewail A H 1996 *J. Am. Chem. Soc.* **118** 8755; Singleton D A, Schulmeier B E, Hang C, Thomas A A, Leung S W and Merrigan S R 2001 *Tetrahedron* **57** 5149
7. Klarner F G, Krawczky B, Ruster V and Deiters U K 1994 *J. Am. Chem. Soc.* **116** 7646; Gajewski J J, Pearson K B and Kagel J R 1987 *J. Am. Chem. Soc.* **109** 5545; Storer J W, Raimondi L and Houk K N 1994 *J. Am. Chem. Soc.* **116** 9675; Houk K N, Lin Y-T and Brown F K 1986 *J. Am. Chem. Soc.* **108** 554; Sakai S 2000 *J. Phys. Chem.* **A104** 922
8. Dinadayalane T C, Vijaya R, Smitha A and Sastry G N 2002 *J. Phys. Chem.* **A106** 1627
9. Geetha K, Dinadayalane T C and Sastry G N 2003 *J. Phys. Org. Chem.* **16** 298; Dinadayalane T C, Punnagai M and Sastry G N 2003 *J. Mol. Struct.* (*Theochem.*) **626** 247; Geetha K and Sastry G N 2003 *Indian J. Chem.* **A42** 11; Dinadayalane T C and Sastry G N 2002 *J. Chem. Soc., Perkins Trans. 2* 1902; Vijaya R, Dinadayalane T C and Sastry G N 2002 *J. Mol. Struct.* (*Theochem.*) **291** 589; Geetha K and Sastry G N 2003 *Indian J. Chem.* **A42** 11; Dinadayalane T C and Sastry G N 2003 *Organometallics* **22** 5526
10. Schmit M W *et al* 1993 *J. Comput. Chem.* **14** 1347
11. Frisch M J *et al* 1998 Gaussian Inc Pittsburgh, PA, Gaussian 98 (Revision A 1)
12. Fukui K 1982 *Science* **218** 747
13. Morao I, Lecea S and Cossio F P 1997 *J. Org. Chem.* **62** 7033; Leces B, Aeeieta A, Roa G, Ugalde J M and Cossia F P 1994 *J. Am. Chem. Soc.* **116** 9613
14. Dinadayalane T C, Punnagai M and Sastry G N 2003 *J. Mol. Struct.* (*Theochem.*) **626** 247; Dinadayalane T C, Geetha K and Sastry G N 2003 *J. Phys. Chem.* **A107** 5479